Ion-acoustic and entropy fluctuations in collisional plasmas measured by laser light scattering

Yi-Quan Zhang and Alan W. DeSilva
Laboratory for Plasma Research, University of Maryland, College Park, Maryland 20742-3511
(Received 10 April 1991)

The ion-acoustic and entropy-fluctuation resonance peaks in the electron-density fluctuation spectrum $S(\mathbf{k},\omega)$ of high-density, low-temperature collisional plasmas (Ar, $T_e=2$ eV, $N_e=1\times10^{17}$ cm^{-3}; He, $T_e=2.3$ eV, $N_e=1\times10^{17}$ cm^{-3}) are measured by means of CO_2 laser scattering. The spectrum consists of three peaks, two due to ion-acoustic waves, and a central entropy-fluctuation peak. The entropy peak (at $\omega=0$) is observed in a plasma. Two theoretical models are introduced, and their predictions compared with the observations. A two-species BGK kinetic model includes the collisional interactions between ions and electrons, which predicts the fluctuation spectrum better than the BGK model, not including the ion-electron collisional interactions. Alternatively, Braginskii's two-fluid transport equations may be used with the fluctuation-dissipation theorem to derive an analytic expression for the fluctuation spectrum, which gives the relation of the thermal transport coefficients to the spectrum. The prediction of Braginskii's equations is used to estimate the transport coefficients experimentally by least-squares fitting the theory to the experiment. The effects on the spectrum of the second-stage ionization species in the plasmas are estimated wtih a three-fluid model.

I. INTRODUCTION

The study of the fluctuations in a plasma is involved fundamentally in the analysis and description of the physical properties of the plasma. The fluctuations are usually characterized by spectral functions, which represent their power spectra. As we will see, the electron-density fluctuation spectrum contains information of correlations among the particles, and is closely related to the transport properties in the plasma. Most important, the electron-density fluctuation spectrum is a quantity that can be directly measured in the laboratory.

Collision-dominated plasmas exist in nature (stellar photospheres, white dwarfs, gaseous planets) and in laboratories (arc plasmas, laser-produced plasmas). Theories have been developed by many authors to include the effects of collisions that do not agree in their predictions of the electron-density fluctuation spectrum. Some of them predict the existence of an enhanced ion-acoustic resonance peak and a zero-frequency entropy peak in the spectrum and others do not. It becomes quite necessary to compare the theories with experimental data.

In the previous work [1,2], the enhanced ion-acoustic resonance peaks in the electron fluctuation spectrum of collisional argon and helium plasmas (with equal ion and electron temperatures) were measured. It was there confirmed that in a collision-dominated plasma, the collision processes will reduce the efficiency of Landau damping and enhance the ion-acoustic fluctuation resonance, which is heavily damped in a collisionless plasma having $T_e\approx T_i$. The entropy fluctuation peak, however, was not observed because of the limitation in the experimental instrumentation.

In the collisional case where Landau damping is not dominant, the fluctuation processes may be sensitive to the thermal transport properties of the plasma. For instance, the shape of the entropy-fluctuation peak may be closely related to the thermal conductivities as with an ordinary fluid. In this work we attempt to examine the existence of the entropy-fluctuation resonance peak experimentally, and to study the relations between the fluctuation spectrum and the thermal transport coefficients of a collisional plasma. A preliminary report of this work has been published [3].

In order to relate the thermal transport coefficients to the fluctuation spectrum, a fluid theory may be adopted. It has been verified that a one-fluid model makes a moderately good fit to the ion-acoustic resonance peaks in the experimental fluctuation spectrum [1,2]. However, the one-fluid theory does not include the interactions between ion and electron species. Braginskii's transport equations [4] solve the problem. In this work, the spectrum is solved from Braginskii's equations in order to compare the Braginskii theory with the experimental data, and to relate the thermal transport coefficients to the experimental data.

The theory of the electron-density fluctuation spectrum is introduced in Sec. II. The fluctuation spectrum is further derived from Braginskii's transport equations and a two-species Bhatngar-Gross-Krook (BGK) model. Three-fluid theory is also discussed. Section III introduces the principle of the light scattering experiment, describes the light scattering conditions in this experiment, and presents the experiment arrangement. The final experimental results of the electron fluctuation spectrum of collisional plasmas are presented in Sec. IV. It contains the comparison of the theories to the experiment, data analysis to obtain the experimental values of the thermal transport coefficients, and a discussion on the effects of Ar^{2+} on the fluctuation spectrum.

II. THEORY OF THE ELECTRON-DENSITY FLUCTUATION SPECTRUM

For a homogeneous and stationary plasma, the electron-density fluctuation spectrum is defined as

$$S(\mathbf{k},\omega)\equiv \lim_{T,V\to\infty}\frac{1}{TV}\frac{\langle n_e(\mathbf{k},\omega)n_e^*(\mathbf{k},\omega)\rangle}{n_0} ,$$

where n_0 is the electron density in thermal equilibrium, T and V are, respectively, the time and volume in which the average process is taken, and $n_e(\mathbf{k},\omega)$ is the Fourier-transformed electron density. Generally, it is a very complicated problem to solve the fluctuation spectrum for a strongly correlated particle system.

The fluctuation-dissipation theorem [5–7] which rigorously connects the power spectrum of the fluctuation to the relevant response function for a system in thermal equilibrium is a powerful tool in simplifying the calculation of the density fluctuation spectrum in a plasma near thermal equilibrium. The form of the fluctuation-dissipation theorem for the electron-density fluctuation spectrum can be expressed as [1,2]

$$S(k,\omega)=\frac{Tk^2}{\pi\omega^2e^2n_0}\mathrm{Re}[\sigma(\mathbf{k},\omega)] ,$$

where σ is an appropriate ac electric conductivity that describes the electron current responding to a fictitious external electric field which only couples to the electrons. Calculation of the conductivity is usually simpler than direct derivation of the fluctuation spectrum.

To implement the calculation of the electric conductivity one might assume that beside the induced electric field governed by Poisson's equation

$$\nabla\cdot\mathbf{E}_{\mathrm{in}}=4\pi\sum_a\rho_a ,$$

there is an external electric field which couples only with the electron species. The conductivity is derived by computing the electron current responding to that external field.

A. BGK equations

The collision term introduced by Bhatngar, Gross, and Krook [8] enables us to solve problems in a collisional plasma in a simple fashion, in which two-particle collisions dominate the discrete interaction processes.

The BGK model is not restricted to any particular collisional regime. It requires use of an arbitrarily selected collision frequency.

A typical BGK equation (with the magnetic field $B=0$) is written as

$$\left[\frac{\partial}{\partial t}+\mathbf{v}\cdot\frac{\partial}{\partial\mathbf{r}}+\frac{q_a\mathbf{E}}{m_a}\cdot\frac{\partial}{\partial\mathbf{v}}\right]f_a=-\frac{1}{\sigma_{aa}}(n_af_a-n_a^2F_{0a}) , \tag{1}$$

where $n_a^0/\sigma_{aa}=v_{aa}$ is the a-a particle collision frequency, n_a is the particle density of species a, and n_a^0 is the undisturbed density of species a. The particle velocity distribution relaxed from collisions, F_{0a}, may be assumed to be Maxwellian:

$$F_{0a}=\left[\frac{m_a}{2\pi T_a}\right]^{3/2}\exp\left[-\frac{m_a(\mathbf{v}-\mathbf{u}_a)^2}{2T_a}\right] . \tag{2}$$

Equations (1) and (2) were linearized, and the electron-density fluctuation spectrum was computed from the linearized equations with help of the fluctuation-dissipation theorem by Mostovych [1,2]. In that work, the only coupling of ions to electrons is through the electric field.

In order to include the effects of the collisional interactions between ions and electrons, an extension of Eqs. (1) and (2) was made to include cross-collision terms between the two species. For this purpose, the following collision terms may be considered:

$$\left.\frac{\partial f_a}{\partial t}\right|_c=-\frac{1}{\sigma_{aa}}(n_af_a-n_a^2F_{0a})-\frac{1}{\sigma_{ab}}(n_bf_a-n_an_bF'_{0a}) , \tag{3a}$$

where

$$F_{0a}=\left[\frac{m_a}{2\pi T_a}\right]^{3/2}\exp\left[-\frac{m_a(\mathbf{v}-\mathbf{u}_a)^2}{2T_a}\right] , \tag{3b}$$

$$F'_{0a}=F'_{0a}(f_a,f_b) , \tag{3c}$$

$$\frac{n_a^0}{\sigma_{aa}}=\nu_{aa} , \tag{3d}$$

$$\frac{n_b^0}{\sigma_{ab}}=\nu_{ab} . \tag{3e}$$

n_a^0 and n_b^0 are the particle densities of species a and b at thermal equilibrium. ν_{aa} and ν_{ab} are the a-a and a-b particle Coulomb collision frequencies, respectively. The relaxation distribution function F'_{0a} is a function of both distribution functions f_a and f_b. To be analogous to the expression of F_{0a} in Eq. (3) we may simply let

$$F'_{0a}=\left[\frac{m_a}{2\pi T'_a}\right]^{3/2}\exp\left[-\frac{m_a(\mathbf{v}-\mathbf{u}'_a)^2}{2T'_a}\right] . \tag{4}$$

The mean velocity $\mathbf{u}'_a$ and temperature T'_a are, in turn, related to the conditions of the particles of species a and b before collisions. In order to establish a model involving the effects of energy transfer (ΔQ_{ab}) and momentum transfer (ΔM_{ab}) between ion and electron species as a result of collisions, we may adopt the following momentum and energy exchange rates [9] to estimate the relaxation temperature T'_a and mean velocity $\mathbf{u}'_a$:

$$\Delta\mathbf{M}_{ab}=\nu_{ab}n_am_a(\mathbf{u}_b-\mathbf{u}_a) , \tag{5a}$$

$$\Delta Q_{ab}=\frac{3\nu_{ab}n_am_a(T_b-T_a)}{m_a+m_b} . \tag{5b}$$

With the aid of Eqs. (5), we may assume

$$\mathbf{u}_a' = \mathbf{u}_b \ , \tag{6a}$$

$$T_a' = T_a + \frac{2m_a}{m_a+m_b}(T_b - T_a) \ . \tag{6b}$$

Equations (3)–(6) along with Poisson's equation

$$\nabla\cdot\mathbf{E}_{\rm in} = 4\pi\sum_a q_a n_a \tag{7}$$

form a closed set of equations of a two-species BGK model. Linearizing the two-species equations, then making a Fourier transform to $\mathbf{k},\omega$ space, yields

$$\begin{aligned}
-i\omega f_i^1 + ikv_\parallel f_i^1 &= \nu_{ii}\left[n_i^1 - f_i^1 + \frac{m_i}{T_0}v_\parallel u_i + \left[\frac{m_i v^2}{2T_0} - \frac{3}{2}\right]\tau_i\right] \\
&\quad + \nu_{ie}\left[n_i^1 - f_i^1 + \frac{m_i}{T_0}v_\parallel u_i' + \left[\frac{m_i v^2}{2T_0} - \frac{3}{2}\right]\tau_i'\right] + \frac{ev_\parallel E_{\rm in}}{T_0} \ , \\
-i\omega f_e^1 + ikv_\parallel f_e^1 &= \nu_{ee}\left[n_e^1 - f_e^1 + \frac{m_e}{T_0}v_\parallel u_e + \left[\frac{m_e v^2}{2T_0} - \frac{3}{2}\right]\tau_e\right] \\
&\quad + \nu_{ei}\left[n_e^1 - f_e^1 + \frac{m_e}{T_0}v_\parallel u_e' + \left[\frac{m_e v^2}{2T_0} - \frac{3}{2}\right]\tau_e'\right] - \frac{ev_\parallel(E_{\rm in}+E_{\rm ex})}{T_0} \ , \\
E_{\rm in} &= \frac{4\pi e n_0}{ik}(n_i^1 - n_e^1) \ ,
\end{aligned} \tag{8}$$

where we have defined

$$f_a = n_a^0 f_a^0(1+f_a^1) \ ,$$
$$n_a = n_a^0(1+n_a^1) \ ,$$
$$T_a = T_0(1+\tau_a) \ ,$$
$$T_a' = T_0(1+\tau_a') \ ,$$

and assumed that f_a^0 is Maxwellian, where $a = i,e$. In order to calculate the approximate electrical conductivity required by the fluctuation-dissipation theorem, the external disturbance field $E_{\rm ex}$ is only inserted in the electron species. In the equations, $V_\parallel = \mathbf{k}\cdot\mathbf{v}/k$, and we assume $\mathbf{E}_{\rm ex}\|\mathbf{k}$. A singly ionized plasma ($z=1$, $n_0 = n_i^0 = n_e^0$) with equal ion and electron temperatures ($T_0 = T_i^0 = T_e^0$) is assumed. The electron mean velocity $\mathbf{u}_e$ may be calculated from Eqs. (8) by using the moment technique with the aid of the following integral expressions of the moments:

$$n_a^1 = \int d^3v f_a^1(\mathbf{k},\omega,\mathbf{v}) f_a^0(\mathbf{v}) \ , \tag{9a}$$

$$u_a = \int d^3v f_a^1(\mathbf{k},\omega,\mathbf{v}) f_a^0(\mathbf{v}) v_\parallel \ , \tag{9b}$$

$$\frac{3T_0}{m_a}(\tau_a + n_a^1) = \int d^e v f_a^1(\mathbf{k},\omega,\mathbf{v}) f_a^0(\mathbf{v}) v^2 \ . \tag{9c}$$

The mean velocity u_e is computed numerically with the moment technique, and the ac electric conductivity thus is obtained by

$$\sigma(\mathbf{k},\omega) = -\frac{eu_e(\mathbf{k},\omega)}{E_{\rm ex}} \ . \tag{10}$$

The fluctuation-dissipation theorem is then applied to produce the fluctuation spectrum.

The spectrum predicted by the two-species model [plotted in Fig. 1(a)] indicates the existence of both ion-acoustic resonance peaks and zero-frequency entropy peak. Comparison of the prediction to that of Eq. (1) shows that both the entropy peak and ion-acoustic resonance peaks are broadened when the ion-electron collisional interactions are introduced [Fig. 1(b)]. The broadening of the entropy peak may be interpreted as a faster decay of the ion temperature fluctuations caused by electron-ion collisions, in which the electrons act like a heat sink to the fluctuations. This broadening becomes more significant in frequency spectra with smaller k vectors, as expected, because the heat sink efficiency becomes more significant in contrast to the heat diffusion in ion species, which tends to become weaker when the k vector is smaller.

Although the two-species BGK model satisfies all of the conservation laws for density, momentum, and energy it still does not include the effects of the detailed structure of the distribution functions f_i and f_e, e.g., their gradients with respect to $\mathbf{v}$ and $\mathbf{r}$. Furthermore, the BGK collision term is developed for the cases of two-particle collisions and may no longer be suitable for a very strong correlation case where three or more particle collisions are found important. As a result, imperfection of its predictions may be expected.

B. Fluid theory — Braginskii's transport equations

Besides kinetic theories, the fluid equations can also be adopted to describe the electron-density fluctuation spectrum of a highly collisional plasma. As a Fourier transform of the dynamic pair correlation function, the fluctuation spectrum contains considerable information on thermal transport processes in a plasma. A significant advantage of a fluid theory over the kinetic theories is that it includes the transport coefficients explicitly and provides a direct way to relate the fluctuation spectrum

to the transport coefficients.

For a plasma with the frequency of the slowest collision processes (e.g., ion-ion collisions) exceeding the highest fluctuation frequency in the ion-acoustic features, the fluid equations become applicable to compute the ion feature of the electron-density fluctuation spectrum. (For a plasma with small plasma parameter $g \equiv 1/n\lambda_D^3$, where n is the particle density, λ_D is the Debye length, this condition can be loosened.) The fluid equations do not take account of mechanisms dependent on microscopic quantities, such as Landau damping, and so are restricted to applications where Landau damping is insignificant.

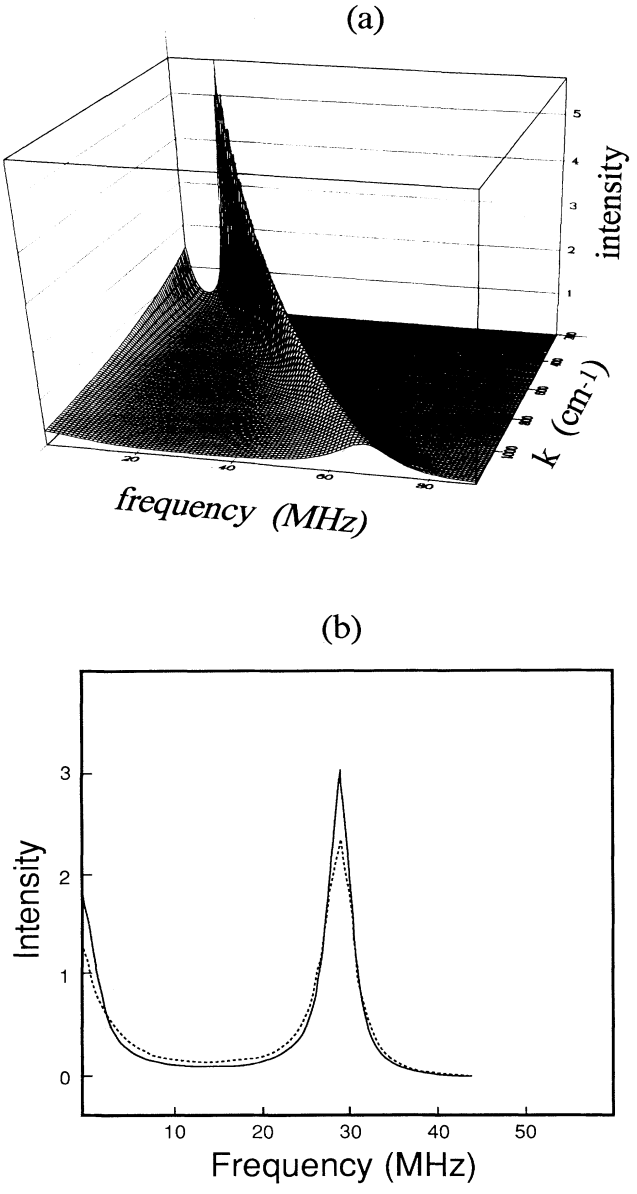

FIG. 1. (a) Scattered light spectrum from two-species BGK model, for argon plasma, with $N_e = 1\times10^{17}$ cm^{-3}, $T_e = 2$ eV. The prominent peak is the ion-acoustic resonance, and the lower peak at zero frequency is the entropy peak. (b) Solid line: spectrum from BGK model with no ion-electron collisional interaction. Dashed line: effect of including ion-electron collisions. **k** represents wave vector, and intensity scale is arbitrary.

The efficiency of the Landau damping is sensitive to the collision frequency of the particles. Higher collision frequencies will enhance the probability of removing a particle from resonance with the potential waves, hence reducing the efficiency of the Landau damping. A computer simulation made to estimate the efficiency of the Landau damping shows that under the condition

$$\nu \gg \omega_s \ ,$$

Landau damping becomes negligible. Here ν is the collision frequency of particles, and ω_s is the acoustic frequency.

We may attempt to derive the electron-density fluctuation spectrum from Braginskii's transport equations [4]. A linearized version of the Braginskii equations for a singly ionized plasma in the absence of a magnetic field can be written as follows.

(i) momentum equations:

$$i\omega m_e n_0 v_e - ik(n_e + n_0 T_e) - \tfrac{4}{3}\eta_e^0 k^2 v_e - e n_0 E^{(e)} + \left[-\frac{m_e n_0}{\tau_e} u - 0.71 ik n_0 T_e \right] = 0 \ ,$$

$$i\omega m_i n_0 v_i - ik(n_i + n_0 T_i) - \tfrac{4}{3}\eta_i^0 k^2 v_i + e n_0 E^{(i)} - \left[-\frac{m_e n_0}{\tau_e} u - 0.71 ik n_0 T_e \right] = 0 \ ,$$

(ii) energy equations:

$$\tfrac{3}{2} i\omega n_0 T_e - ik n_0 T_0 v_e - ik(0.71 n_0 T_0 u - ik\kappa^e T_e) - \frac{3m_e}{m_i}\frac{n_0}{\tau_e}(T_e - T_i) = 0 \ , \quad (11)$$

$$\tfrac{3}{2} i\omega n_0 T_i - ik n_0 T_0 v_i - k^2 \kappa^e T_i + \frac{3m_e}{m_i}\frac{n_0}{\tau_e}(T_e - T_i) = 0 \ ,$$

where n_0 is the electron density at equilibrium, and τ_e, κ^e, κ^i, and η_0^i are the electron collision time, electron thermal conductivity, ion thermal conductivity, and ion viscosity coefficient, respectively. The fluctuation components of the ion mean velocity, electron mean velocity, ion temperature, and electron temperature are represented as $v_i(k,\omega)$, $v_e(k,\omega)$, $T_i(k,\omega)$, and $T_e(k,\omega)$, respectively, and u is the mean relative velocity between electron and ion species:

$$u = v_e - v_i \ .$$

In order to apply the fluctuation-dissipation theorem in the derivation, the electric fields $E^{(i)}$ and $E^{(e)}$ are assigned in the following ways:

$$E^{(e)} = E_{\rm in} + E_{\rm ex} \ ,$$
$$E^{(i)} = E_{\rm in} \ , \quad (12)$$
$$E_{\rm in} = \frac{4\pi n_0 e}{i\omega}(v_i - v_e) \ .$$

In order that we may derive the response function of the electrons to the external field, the fictitious external field E_{ex} is only allowed to interact with the electron species. The fluctuations of the ion species are reflected in the fluctuations of the electron species through the collective interactions between the two.

An exact analytic expression for the spectrum may be derived, but it is very complicated. Under the conditions of low frequency and long wavelength [$\omega \leq kC_s$, $k \ll k_D$, where $C_s=(T/m_i)^{1/2}$ is the ion-acoustic velocity, and k_D is the Debye wave vector], and in the absence of a magnetic field, the spectrum may be approximated as

$$S(\mathbf{k},\omega)=n_e\frac{A(k)+B(k)\beta^i/D(k,\omega)}{[A(k)+B(k)\beta^i/D(k,\omega)]^2\omega^2+[2-\omega^2/\omega_0^2+\frac{3}{2}B(k)\omega^2/D(k,\omega)]^2}\ , \tag{13}$$

where

$$A(k)=\frac{n_e}{k^2\kappa^e}+\frac{4}{3}\frac{\eta_0^i}{n_eT}\ ,$$

$$B(k)=\frac{n_e}{k^2\kappa^e}C_{ie}+1\ ,$$

$$D(k,\omega)=(\beta^i)^2+(\tfrac{3}{2}\omega)^2\ ,$$

and

$$\beta^i=\frac{k^2\kappa^i}{n_e}+C_{ie}\ ,$$

$$\omega_0=k(T/m_i)^{1/2}\ .$$

$C_{ie}=3m_e/m_i\tau_e$ is the collisional energy-transfer frequency between the ions and electrons, τ_e is the electron collision time, n_e is the electron density, and κ^i, κ^e, and η_0^i are the ion and electron thermal conductivities, and ion viscosity coefficient, respectively.

The spectrum predicted by the Braginskii equations for a high-density, low-temperature plasma is plotted in Fig. 2 predicting the existence of both the ion-acoustic peak and the entropy peak.

The computational result shows that in the entropy-fluctuation frequency region, the high electron thermal conductivity prevents the electron temperature from fluctuating significantly compared with the ion temperature fluctuation: $|\delta T_e|/|\delta T_i|\leq 0.05$ for the conditions under which the data were measured in this experiment. The damping of the ion entropy fluctuations is mainly due to ion thermal conduction. The collisional interaction between the ion and electron species provides heat transfer between the species. The electron species in this case acts like a heat sink which accelerates the damping of the entropy resonance. The width of the entropy peak is additionally influenced by this damping. In the case of $\beta^i \ll kC_s$ and $k^2\eta_0^i/n_em_i \ll kC_s$, the width of the entropy peak is

$$\delta\omega_{\text{entropy}}=\frac{2}{3+B(k)}\left[\frac{k^2\kappa^i}{n_e}+C_{ie}\right]\ ,$$

where the first term is due to ion thermal conduction, and the second term due to the energy transfer between ions and electrons. For large k, ion thermal conduction will dominate damping because the temperature gradient is proportional to k. When k approaches zero, the width of the entropy peak will reach a constant which is determined by the energy transfer between the ion and electron species.

Under the conditions of $\beta^i \ll kC_s$ and $1/A \gg kC_s$, the ion-acoustic peaks approach Lorentzian forms

$$S(k,\omega)\rightarrow\frac{S_0\Gamma k^2}{(\Gamma k^2)^2+(\omega-\omega_r)^2}\ ,$$

where

$$\Gamma k^2=\frac{A(k)k^2T}{2m_i}+\frac{2B(k)\beta^i}{9[2+\frac{2}{3}B(k)]}\ ,$$

$$\omega_r=\left[2+\frac{2B(k)}{3}\right]^{1/2}\omega_0\left\{1-\frac{4}{27}\frac{B(k)(\beta^i)^2m_i}{[2+2B(k)/3]^2k^2T}-\frac{A(k)}{4[2+2B(k)/3]^2}\left[\frac{4B(k)\beta^i}{9}+A(k)\left[2+\frac{2B(k)}{3}\right]k^2\frac{T}{m_i}\right]\right\}\ ,$$

$$S_0=\frac{n_e}{2+\frac{2}{3}B(k)}\ .$$

Because $A(k)$ is mainly determined by the ion viscosity coefficient η_0^i, the bandwidth of the ion-acoustic resonance peak is mainly determined by η_0^i. The ion thermal conductivity in the second term of the damping parameter Γk^2 also causes an observable effect in the damping of the ion-acoustic resonances.

The electron thermal conductivity may have a perceptible effect on the damping of the entropy and ion-

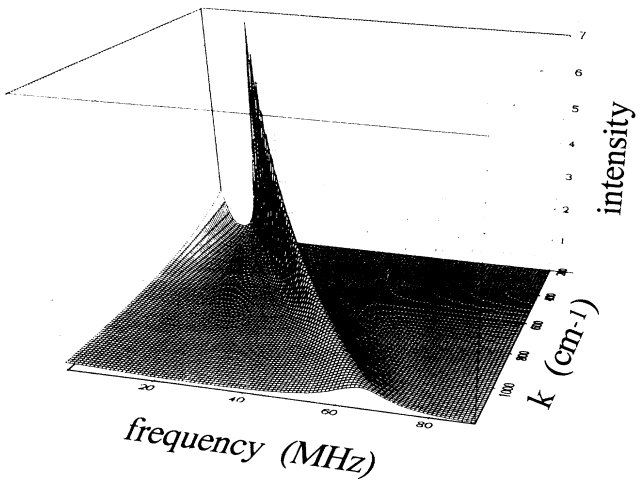

FIG. 2. Scattered light spectra deduced from the Braginskii two-fluid theory, for conditions of Fig. 1.

acoustic resonances when the wave vector k is very small $[k \ll (T/\kappa^e \eta_0^i)^{1/2}]$, in which condition the temperature fluctuations in the electron species may no longer be small in comparison to that of the ion species.

C. Three-fluid problem

When the second-stage ionization in a plasma is not negligible, or when the atoms are not fully ionized, the influences of the doubly ionized particles or the neutral particles on the electron-density fluctuation spectrum may be estimated by adding a third fluid in the fluid theory described previously. For a low-temperature plasma, the symmetrical resonance charge transfers have very large cross sections. Consequently, energy and momentum coupling among the species may become considerable. The influences of the neutral particles and ions in different ionization stages on the density fluctuation spectrum may be detectable when the fractions of these particles in the plasma are significant.

For a plasma involving both singly and doubly ionized ions, Eqs. (11) may be extended to include momentum and energy equations for the double ionization species and to contain the coupling terms that represent the collisional or charge-transfer interactions of the doubly ionized ions with singly ionized ions and electrons. The energy-transfer terms from the double ionization stage fluid to the electron and the singly ionized ion fluids may be given as

$$\Delta E_{2,e} = \frac{3m_e}{m_i} \frac{n_0}{\tau_{e,2}} (T_{i2} - T_e)$$

and

$$\Delta E_{2,1} = \frac{3n_0^{i1}}{\tau_{1,2}} (T_{i2} - T_{i1}) ,$$

where n_0 and n_0^{i1} are the equilibrium particle densities of the electron and singly ionized ion fluids, respectively. T_e, T_{i1}, and T_{i2} denote the temperatures of the electrons, singly ionized ions, and doubly ionized ions, respectively. $\tau_{e,2}$ and $\tau_{1,2}$ are the collision times for momentum transfer between electrons and doubly ionized ions, and between the singly ionized and doubly ionized ions. In the momentum equations, the friction force and thermal force terms arising from the interactions of electrons with doubly ionized ions are similar to those with singly ionized ions. The momentum transfer term between the singly and doubly ionized ion fluids is estimated as

$$\Delta M_{1,2} = \frac{m_i n_0^{i1}}{\tau_{1,2}} (v_{i1} - v_{i2}) ,$$

where v_{i1} and v_{i2} are the mean velocities of the singly and doubly ionized ions, respectively.

In comparison to the spectrum predicted by the two-fluid Braginskii equations, the three-fluid model, which takes into account the influence of the second ionized stage ions, predicts a narrower bandwidth for both the entropy and ion-acoustic resonances. The differences appearing between the predictions can be interpreted as follows. The effective charge number Z of the two ion species is larger than one. This modifies the average ion-ion collision time, hence the average ion thermal conductivity and viscosity coefficient to smaller values. Thus a spectrum with narrower resonance peaks is expected. The effective charge-to-mass ratio of the ion fluid increases when the fraction of second-stage ionization increases. Therefore the ion-acoustic frequency increases.

The three-fluid theory dealing with the neutral particles as the third fluid is similar to that with the second ionization stage ions. Because of smaller interaction cross sections, the influences of the neutral particles on the fluctuation spectrum are not as significant as those of the second ionization stage ions for the well-ionized argon plasma used in this study.

III. LIGHT SCATTERING EXPERIMENT

A. Light scattering method

Light scattering is employed to obtain the fluctuation spectrum. The power in the scattered light may be written as follows [10,11]:

$$Ps(\omega_s) = \frac{ANI_0 r_0^2 |\eta|^2}{\pi R_0^2} S(\mathbf{k}_s - \mathbf{k}_i, \omega_s - \omega_i) , \tag{14}$$

where A is a small area on which the power of the scattered light is measured, R_0 is the distance between the small area A and the light scattering region, and N and I_0 are the total number of electrons involved in the light scattering volume, and the power intensity of the incident light, respectively. $\mathbf{k}_i$ and $\mathbf{k}_s$ are the wave vectors of the incident and scattered waves, and ω_i and ω_s their frequencies, $r_0 = e^2/m_e c^2$ is the classical electron radius, and $\eta = (\mathbf{R}_0/R_0) \times [(\mathbf{R}_0/R_0) \times (\mathbf{E}_i/E_i)]$ where $\mathbf{E}_i$ is the electric field of the incident light. Equation (14) indicates that the power spectrum of the scattered light reveals the electron-density fluctuation spectrum in the plasma.

Because the frequency shift in the scattered light is

very small compared with the frequency of the light, $k_i = k_s$ holds closely, hence the relation among the $\mathbf{k}$ vectors implies in Eq. (14),

$$\mathbf{k} = \mathbf{k}_s - \mathbf{k}_i \ ,$$

where $\mathbf{k}$ is the wave vector of the electron-density fluctuations, shows that k satisfies the Bragg scattering condition

$$k = 2k_i \sin\left[\frac{\theta}{2}\right] \ ,$$

where θ is the scattering angle, the angle between $\mathbf{k}_s$ and $\mathbf{k}_i$. This means that the wave vector of the measured fluctuation spectrum is determined by the wavelength of the incident light and the scattering angle. When a laser beam is adopted as the source light, the limit of the geometric resolution is mainly determined by the divergence of the laser beam, and is of the order

$$\frac{\Delta k}{k} \simeq \frac{\lambda_i}{\pi a_0} \ ,$$

where λ_i is the wavelength of the laser and a_0 is the waist diameter of the laser beam.

B. Heterodyne detection technique

The ion feature of the fluctuation spectrum carried by the scattered light spans only a very tiny band in the light spectrum

$$\frac{kC_s}{\omega_s} \simeq 10^{-6} \ ,$$

and is difficult to resolve with an optical spectroscopic instrument. Furthermore, to filter the stray light from that tiny band of spectrum by optical means is not realistic. The heterodyne technique may be employed to solve this difficulty. This technique is characterized by a significantly better resolution and offers a more convenient environment for signal filtering. When the heterodyne technique is adopted, the scattered light is mixed with a local oscillator light beam. The total electric field is thus written as

$$E_t(t) = E_s(t) + E_{\mathrm{LO}}(t) \ ,$$

where the local oscillator beam and the scattered light fields are expressed as

$$E_{\mathrm{LO}}(t) = E_{\mathrm{LO}} e^{-i\omega_{\mathrm{LO}} t} \ ,$$

$$E_s(t) = \frac{1}{2\pi} \int d\omega \, E_s(\omega) e^{-i\omega t} \ .$$

The mixed signal is detected by a wideband optical detector. The output current of the detector $I_d(t)$ is proportional to the power flux of the detected light

$$I_d(t) = e\sigma |E_T(t)|^2 \ ,$$

where σ is an efficiency of the detector system. The average power spectrum of the detector current can be easily derived and is related to the scattering signal in the following way:

$$\begin{aligned} \lim_{T\to\infty} \frac{1}{T} \langle |I_d(\Omega)|^2 \rangle &= \frac{8\pi^2 e^2 \sigma^2}{cA} |E_{\mathrm{LO}}|^2 [P_s(\omega_{\mathrm{LO}} + \Omega) + P_s(\omega_{\mathrm{LO}} - \Omega)] \\ &= \frac{8\pi e^2 \sigma^2 r_0^2 |\eta|^2 N I_0}{cR_0^2} |E_{\mathrm{LO}}|^2 [S(\mathbf{k}_s - \mathbf{k}_i, \omega_{\mathrm{LO}} - \omega_i + \Omega) + S(\mathbf{k}_s - \mathbf{k}_i, \omega_{\mathrm{LO}} - \omega_i - \Omega)] \ . \end{aligned} \tag{15}$$

The detected spectrum considered so far is an average over infinite detection time. In a real experiment, the detection time is finite, and the signal-to-noise ratio has to be considered. Consider a real data acquisition system. In the system, the total power spectrum in the output of the detector consists of signals $[P_d(\Omega)]$; shot noise $[P_{\mathrm{SN}}(\Omega) = e\langle I_T^0 \rangle / \pi$, where I_T^0 is the dc component of the detector current]; and the noise from other noise sources $[P_n(\Omega)]$:

$$P_T(\Omega) = P_d(\Omega) + P_{\mathrm{SN}}(\Omega) + P_N(\Omega) \ . \tag{16}$$

The signal-to-noise ratio of the power spectrum $P_d(\Omega)$ is estimated by [12]

$$(S/N)_\Omega = \frac{P_d(\Omega)}{P_T(\Omega)} (1 + \delta\Omega T)^{1/2} \ , \tag{17}$$

where $\delta\Omega$ is the bandwidth, and T is the time interval of observation. Averaging the spectrum over N samples and over a rectangular frequency window of bandwidth $n\delta\Omega$, and using the fact that for a Fourier transform $\delta\Omega = 1/T$, the signal-to-noise ratio becomes

$$(S/N)_\Omega = \frac{\bar{P}_d(\Omega)}{\bar{P}_T(\Omega)} (1 + Nn)^{1/2} \ . \tag{18}$$

This relation determines the required number of samples to obtain a given frequency resolution.

Because the signal P_d is boosted by the power of the local oscillator beam proportionally, the ratio P_d/P_{SN} is independent of the power of the local oscillator. If $P_N(\Omega)$ is not dependent on the power flux of the detected light, an increase in the power of the local oscillator beam would improve the signal-to-noise ratio. Unfortunately, the $1/f$ noise, which may strongly depend upon the detector current, will diminish the signal-to-noise ratio in the low-frequency region and may limit the improvement

of the signal-to-noise ratio accomplished by increasing the local oscillator power. To overcome the problems arising from the $1/f$ noise, a laser modulator is adopted to shift the frequency of the local oscillator laser beam, which is originally split from the scattering light source. With an acoustic modulator (Bragg cell) of frequency $\omega_{\rm mod}$, the local oscillator frequency $\omega_{\rm LO}$ in Eq. (15) becomes

$$\omega_{\rm LO}=\omega_i+\omega_{\rm mod} .$$

Thus Eq. (16) is rewritten in the following form:

$$\lim_{T\to\infty}\frac{1}{T}\langle|I_d(\Omega)|^2\rangle \propto [S(\mathbf{k}_s-\mathbf{k}_i,\omega_{\rm mod}+\Omega) + S(\mathbf{k}_s-\mathbf{k}_i,\omega_{\rm mod}-\Omega)] . \quad (19)$$

The fluctuation spectrum in the zero-frequency region is hence represented in the detected spectrum in the frequency region around $\omega_{\rm mod}$, and is separated from the noisy zero-frequency region of the detector system. This makes it possible to measure the zero-frequency entropy-fluctuation components in this experiment.

C. Experimental conditions

Plasma and light source conditions were carefully selected to satisfy the many conditions necessary for the measurement. The condition of high collisionality demands that the ion-ion collision frequency ν_{ii} be greater than the frequency of the fluctuations. This will be met for all frequencies of interest in the ion feature if

$$\nu_{ii} > kC_s ,$$

where C_s is the ion sound speed $(T/m)^{1/2}$, and k the wave number of the fluctuations to be sampled. We may pick the magnitude and direction of k by properly selecting the laser wavelength and direction of incidence. k satisfies the vector relation $k=k_i-k_s$, where subscripts i and s refer, respectively, to the incident and scattered light. If θ is the angle between these rays, the magnitude of k is

$$k=4\pi/\lambda_0\sin(\theta/2) .$$

The ion-ion collision frequency may be expressed

$$\nu_{ii}=4.8\times10^{-8}n\Lambda/T^{3/2}m^{1/2} ,$$

where Λ is the Coulomb logarithm. The above condition hence reduces to

$$\frac{n\Lambda\lambda_0}{T^2\sin(\theta/2)}>2.6\times10^8 .$$

This implies that high-density, low-temperature plasma, large-wavelength scattering light source, and small-angle scattering may be required to fill the condition.

In addition, if the scattered light spectrum is to represent the wave spectrum of the plasma, the scattering parameter $\alpha=1/k\lambda_D$ must be >1 [11]. A further condition is that the frequency of the laser be higher than the plasma frequency so that the radiation will propagate, and that the absorption of the probe radiation be small enough to survive transit through the plasma and its boundary layers. What absorption does occur must be small enough so that the energy deposited does not significantly perturb the plasma under study.

The plasma must be quiet, so that the fluctuations are dominated by thermal excitation, and not by instability, and the plasma lifetime must be long enough so that a good signal-to-noise ratio may be obtained with a reasonable number of shots.

All of these conditions are satisfied by the argon plasma ($n_e=1\times10^{17}$ cm^{-3}, $T_e=2$ eV) used in these studies, in conjunction with a pulsed CO_2 laser which produces a 100-μsec-duration pulse of about 100 W, in single-mode operation.

D. Experiment scheme

The optics of the experiment are shown in Fig. 3. To apply the heterodyne technique, 5% of the CO_2 laser beam is split off to serve as a local oscillator. The frequency of the local oscillator beam is shifted by an acoustic Bragg cell (Model AGM-406B manufactured by Intra Action Corp.). The principal deflected beam from the modulator, which is used as the local oscillator, is Doppler shifted by about 50 MHz, and is attenuated to the desired intensity by a variable attenuator. The resolution of the light scattering measurement is dependent on the divergence of the laser beams at the scattering volume. The divergence angle is related to the size of the laser waist by the relation $\Delta\theta=\lambda_i/\pi a$. The laser waist at the scattering volume can be selected by setting the combined focal lengths of the doublet lenses L_1-L_2 and L_3-L_4. Larger laser waist results in smaller divergence angle and improves the angular resolution of the optical system. However, the overlap region of the main beam and the local oscillator beam with large waists may extend beyond the homogeneous plasma region when the scattering angle is small. Due to the above reasons, the laser waist defining the scattering volume is chosen to be about 0.35–0.5 mm. This gives about 4% angular resolution for 8° light scattering and about 8% resolution for 4° scattering.

The local oscillator beam, along with the scattered

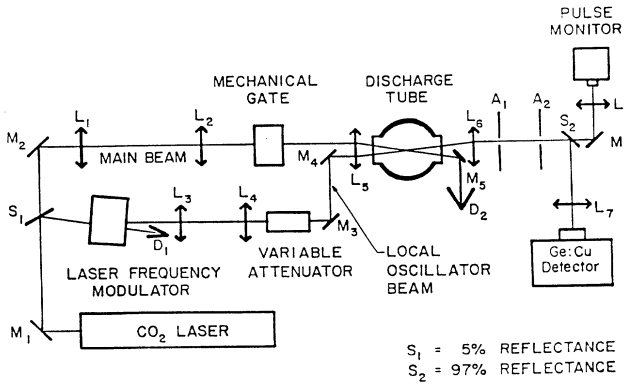

FIG. 3. The optics of the experiment.

light from the plasma in the direction of the local oscillator beam, passes through apertures A1 and A2, and is received by the high-frequency (400 MHz) Ge:Cu liquid-helium-cooled infrared detector.

The electronic system is shown in Fig. 4. Although the stray light component is mostly blocked by the apertures A1 and A2, it is still intense enough to saturate the preamplifier. In addition, because of a very weak sound wave component propagating in the opposite direction in the laser modulator, the deflected light due to this component beating with the main component of the local oscillator beam produces a $2\omega_{\rm mod}$ signal which will also saturate the preamplifier. In order to avoid the signal saturation, the detected photocurrent is first passed through a set of notch filters with center frequencies about 50 and 100 MHz, which attenuate these spurious components to an acceptable level. Next, the signal is filtered by a 5-MHz high-pass filter and is amplified by an ultra-low-noise preamplifier (Miteq Model AU-3A-0150, noise figure of 1.4 dB, gain of 46 dB, and frequency bandwidth 1–500 MHz). The signal is further amplified to a peak-to-peak amplitude of about 300–400 mV before being digitized by an ultrafast wave-form digitizer (Le Croy Model 6880, 1.35 G samples/sec sampling rate). The noise figure of the overall electronic system is measured to be about 2.1 dB. The maximum time window of the digitizer is 7.43 μsec, or 10^4 samples. The digitized wave-form data are transferred to a microcomputer and the frequency spectra are extracted from the wave-form data by digital Fourier transform signal processing software.

In order to obtain the desired results, one has to distinguish the scattering signal from the detector noise and to determine the gain factor of the overall detection system. The following measurements have to be made: (1) the total signal $P_T(\omega)$, which includes the scattering signal, detector current noise, and the noise from the electronic system, (2) the detector noise $P_N^d(\omega)$ and the electronic system noise $P_N^0(\omega)$ only, $P_N(\omega)=P_N^d(\omega)+P_N^a(\omega)$, which is measured when the main laser beam (scattering light source) is off; (3) the noise from the electronic system only, $P_N^a(\omega)$, which is measured when both the main laser beam and the local oscillator beam are off; and (4) a white noise spectrum $P_{\rm WN}(\omega)$, which is measured for the purpose of normalization. The white noise spectrum is obtained by taking the difference between the noise spectra of a 1-kΩ resistor, which is in place of the laser detector, at two different temperatures (liquid-nitrogen temperature and room temperature). Finally the fluctuation spectrum in relative amplitude units can be expressed by

$$\langle P_s(\omega)\rangle=\frac{\langle P_T(\omega)\rangle-\langle P_N(\omega)\rangle}{\langle P_{\rm WN}(\omega)\rangle}\ , \tag{20}$$

where the angular brackets express the average over many shots, which is required to achieve a reasonable signal-to-noise ratio.

The condition under which the white noise $P_{\rm WN}(\omega)$ is measured may still not be identical to the condition in the light scattering experiment, though care was taken to make them the same. The reflections of the high-frequency signals in the electronic system may hence differ from each other and may produce different ripple patterns in the gain factor of the overall electronic system. To reduce the possible errors arising in this case, the expression for the final resultant spectrum is modified as follows:

$$\langle P_s d(\omega)\rangle=\frac{\langle P_T(\omega)\rangle-\langle P_N(\omega)\rangle}{\langle P_N(\omega)\rangle-\langle P_N^a(\omega)\rangle}N(\omega)\ , \tag{21}$$

where $N(\omega)$ is a normalization function given as

$$N(\omega)=a+\frac{b}{\omega}\ ,$$

where the first term is the shot-noise term, and the second one is the $1/f$ noise term. The parameters a and b are determined by a least-squares fit to the ratio of the detector noise to the white noise, $\langle P_N^d(\omega)\rangle/\langle P_{\rm WN}(\omega)\rangle$. Equation (21) will provide an accurate result when the condition under which $P_N(\omega)$ is measured is close to that under which $P_{\rm WN}(\omega)$ is measured. The ratio $\langle P_N^d(\omega)\rangle/\langle P_{\rm WN}(\omega)\rangle$ is examined in this experiment and the measurement shows a very smooth $1/f$ noise plus a small shot-noise component.

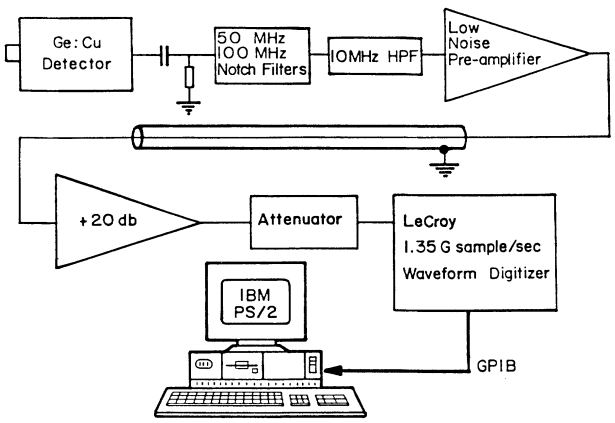

FIG. 4. Data acquisition system.

IV. SCATTERING RESULTS AND CONCLUSIONS

The electron-density fluctuation frequency spectra have been measured for wave vectors of from 300 to 1000 $\rm cm^{-1}$ and frequencies of 1 to about 85 MHz in the argon plasma ($N_e=1\times10^{17}$ $\rm cm^{-3}$, $T_e=2$ eV). In addition, the spectra ($k=489$ and 807 rad/cm, and frequency of 5 MHz–330 MHz) have also been observed in the helium plasma ($N_e=1\times10^{17}$ $\rm cm^{-3}$, $T_e=2.3$ eV). The plasma conditions in this experiment were determined independently of scattering, by interferometry and spectroscopic measurements [2]. They are listed in Table I. The frequency difference between the main laser beam and the local oscillator beam is fixed at 52 MHz for the measurements in the Ar plasma and at 0 in that of the He plasma.

The final scattering spectrum is obtained by the data processing described in the preceding section. The experimental results of the fluctuation spectra are shown in Figs. 5 and 6.

TABLE I. The plasma conditions in this experiment. (P_{fill} is the fill pressure, V_d is the discharge voltage of the capacitor bank. Measured by Mostovych [1]).

	Argon	Helium
P_{fill} (torr)	3	7
V_d (V)	1500	1500
N_e (cm^{-3})	$(1.025\pm0.050)\times10^{17}$ cm^{-3}	$(0.95\pm0.05)\times10^{17}$ cm^{-3}
T_e (eV)	$1.95^{+0.20}_{-0.11}$	$2.3^{+0.4}_{-0.2}$
λ_D (cm)	3.28×10^{-6}	3.56×10^{-6}
g ($\equiv 1/n\lambda_D^3$)	0.28	0.22
ν_{ii} (sec^{-1})	1.96×10^{9}	4.8×10^{9}

The measured fluctuation spectra in the Ar and He plasma present ion-acoustic resonance peaks, which would be heavily damped in a collisionless plasma, and a zero-frequency entropy peak. Because the frequency of the local oscillator is shifted 52 MHz by a laser modulator in the measurement of the argon plasma, the acquired spectra in the experiment with the Ar plasma have been shifted and the central zero-frequency peaks, which are due to the entropy fluctuations, appear at the position of 52 MHz in the data acquisition system. The peaks appearing at the two sides are due to ion-acoustic waves propagating in opposite directions. The spectra obtained from larger angle scattering, e.g., scattering at angles of 9° or 10° in the argon plasma, seen to be unsymmetrical because the left-hand-side peaks fall in the frequencies close to the zero frequency of the detector output, so their remote wings are folded over and added into their

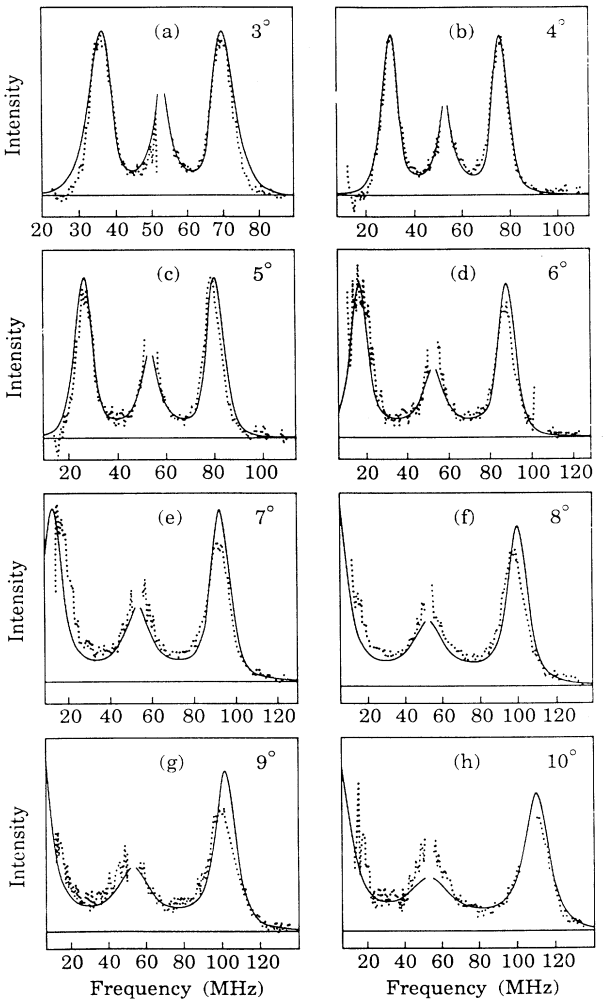

FIG. 5. Measured scattered light spectra (dots), and predictions of the two-fluid theory, for argon plasmas, under conditions of Figs. 1(a)–1(h) are the spectra for scattering angles of 3°–10°. For scattering angles above about 7°, the spectrum is broad enough so that the low-frequency wing is folded back around zero frequency.

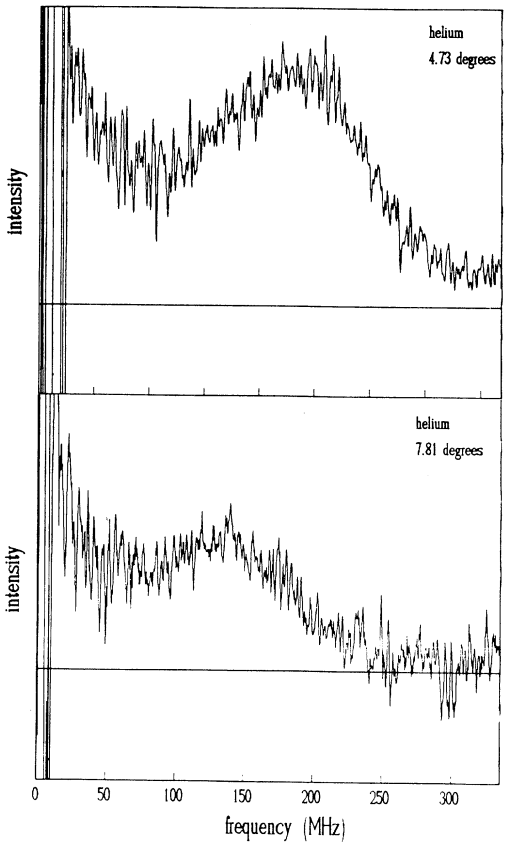

FIG. 6. Measured scattered light spectra for helium plasmas, for $N_e=1\times10^{17}$ cm^{-3}, $T_e=2.3$ eV. System noise becomes very large below 10 MHz.

inner wings [see Eq. (19)].

The ion-acoustic resonance peak in collisional plasmas has been observed in previous work [2]. This resonance would be enhanced for the condition $T_e/T_i \gg 1$, and/or may also be driven by the discharge current. Full discussion has been made by Mostovych and De Silva [2] to verify that these are very unlikely in the plasmas used in this experiment. The very high collision frequency of these plasmas ensures near equality of T_e and T_i. Mostovych's research verified that the discharge current enhanced the ion-acoustic waves in the direction of the current by about 20%, but no effect of the current could be seen for the directions perpendicular to the current (the condition under which data were taken).

The entropy-fluctuation peak is well known in an ordinary fluid. However, this is an observation of the entropy-fluctuation resonance peak in a plasma. While the ion-acoustic resonance waves are pressure (mechanical) fluctuation waves, the entropy fluctuation is associated with the temperature fluctuation which is not propagating (hence producing a zero-frequency peak) and decays mainly through the heat diffusion process. The ion-acoustic resonance waves damp mainly by the viscosity in the ion species when the Landau damping is not important (which happens in a collision-dominated plasma). So, in a collisional plasma, the shapes of the electron fluctuation spectrum may contain information about the thermal transport properties in the plasma.

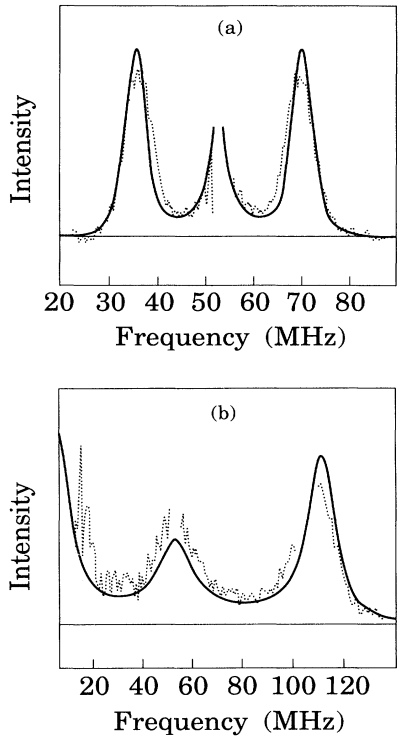

FIG. 7. Measured scattered light spectra for argon plasmas compared with predictions of the two-species BGK model. (a) 3° scattering angle ($k = 310$ cm^{-1}). (b) 10° degree scattering angle ($k = 1033$ cm^{-1}).

A. Comparison of the theories to the experiment

Solid lines superposed in Fig. 5 are the spectra predicted by Braginskii's transport equations, using independently measured electron density and temperature, convolved with the instrumental function for purposes of comparison with experiment. For the Ar plasma, the theory fits to the experiment reasonably well for small-angle scattering (3°, 4°, and 5°). However, the following major departures of the theory from the experiment become significant when the scattering angle increases: The theory gives broader entropy-fluctuation peaks; and the ion-acoustic peaks predicted by the Braginskii theory are narrower than those observed by the experiment.

Supposing that Braginskii's theory used in the two-fluid modeling is valid in the plasmas in this experiment, these departures may be interpreted as indicating that the ion thermal conductivity predicted by the theory is larger than the measured value, and that the ion viscosity coefficient is smaller than the measured value. The difference between theoretical and experimental values of the ion-acoustic frequency is still within the error bar of the theoretical value caused by the uncertainties in measurement of the temperature and the scattering angle ($\pm 0.15°$).

The spectra predicted by the two-species BGK model are plotted in Fig. 7, and give broader entropy-fluctuation and ion-acoustic peaks in comparison to the predictions of the simple BGK without collisional interactions between ion and electron species, and fit the experimental data better than the simple BGK model. The spectrum predicted by the two-species BGK model fits the experimental data closely. However, the widths of the ion-acoustic peaks predicted by the BGK theory are narrower than those observed in the experiment, especially for those spectra with large wave vectors.

The experimental spectra obtained from the helium plasma (Fig. 6) show that the ion-acoustic resonance peaks are significantly broader than those predicted by Braginskii's equations. In the helium plasma, the Landau damping will be slightly more significant than in the Ar plasma in the conditions in this experiment. The additional broadening owing to the Landau damping is estimated to be at most 1 MHz for the spectrum with $k = 489$ rad/cm, which is still negligible in comparison to the width of the ion-acoustic peak in the spectra of the helium plasma. The helium plasma in this experiment, however, is not quite stable. The broad ion-acoustic resonance peaks in the helium plasma may be related to the average of the fluctuation spectra over flickering conditions in the plasma.

Of all the theories, the predictions of Braginskii's transport equations and the two-species BGK model make the best fit to the experiment. The theories, such as Grewal's model, which predict only a single zero-frequency peak, of course are poor theories for the collision-dominated plasmas.

B. Relations to the thermal transport coefficients

The spectrum derived from the Braginskii transport equations gives the relations between the thermal trans-

port coefficients and the spectrum. The Braginskii equations are derived for a plasma in which small-angle collisions are the most probable events. Thus these equations may not be strictly applicable when the plasma parameter g is no longer small. The value of g in this experiment is about 0.3, which is moderately small, but does not fit the condition $g \ll 1$ satisfactorily. Supposing that the transport equations, considered as a two-fluid theory, are valid for the plasma in our experiment, and that the discrepancies between theory and experiment are due to the imperfect models for the transport coefficients, we may perform a least-squares-fitting procedure to fit the theoretical spectrum to the experimental data, in which the transport coefficients are treated as variables to be determined by the fit. Equations (13) are accordingly fitted to the experimental spectra of the Ar plasma by least-squares fitting, with the parameters κ^i, κ^e, η_0^i, C_{ie}, C_s $(=\omega_0/k)$, and the amplitude scales of the spectra allowed to vary. The fitted spectra are indicated by the solid lines in Fig. 8. The resultant parameters are listed and compared with Braginskii's values in Table II.

The resultant values of ion thermal conductivity κ^i and ion viscosity coefficient η_0^i from the fitting are about 30% smaller and 40% greater than Braginskii's predictions, respectively. The resultant values of ion-acoustic speed C_s and the collisional electron-ion energy-transfer frequency C_{ie} agree reasonably with Braginskii's values. The experimental value of the electron thermal conductivity κ^e with about 60% relative error is about twice the value predicted by Braginskii.

Because the spectrum is not sensitive to the electron thermal conductivity, κ^e cannot be determined well by the fitting process, as is seen by its large error bar. The heat diffusion rate is proportional to the gradient of the temperature which is proportional to the magnitude of the wave vector k. The heat diffusion time scale in a periodical entropy wave is proportional to the wavelength, which is again of the magnitude $1/k$. The overall heat diffusion time scale is then proportional to $1/k^2$. In the electron species, the heat diffusion time scale is very short when the wave vector k is not very small, owing to a large electron thermal conductivity. The electron species acts like a heat sink with uniform temperature, and the effect of the change in the electron thermal conductivity on the fluctuating waves becomes insignificant. In order to estimate the electron thermal conductivity precisely, smaller scattering angles or/and longer-wavelength probing radiation may be required to obtain spectra with smaller wave vector k, in which the effect from electron thermal conduction may become

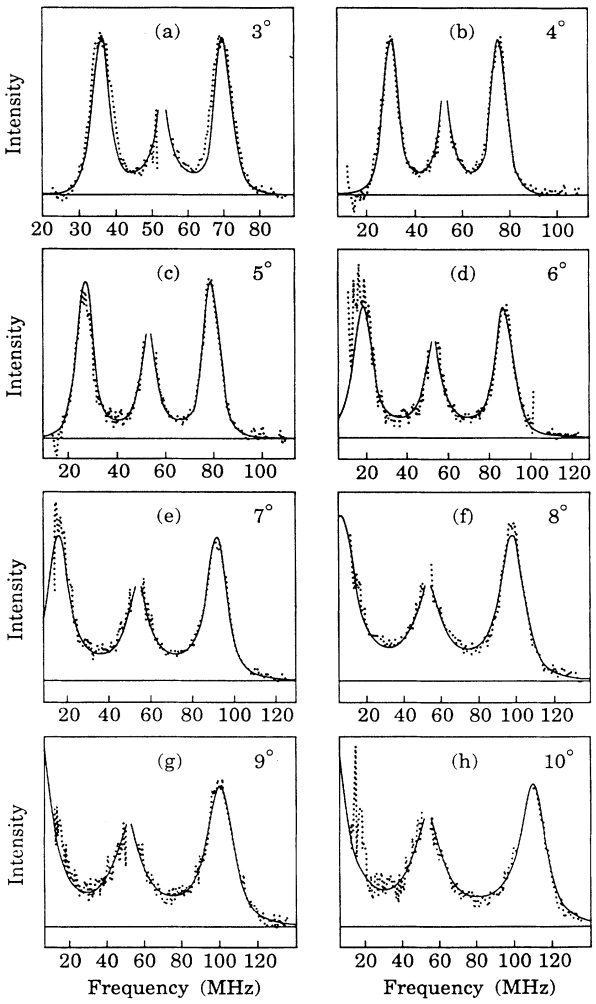

FIG. 8. Data of Fig. 5, fitted by adjusting transport coefficients in the two-fluid theory.

significant. Problems will arise in the measurement of the spectrum with a scattering angle less than 2° in this experiment because of the ultrabright stray light environment.

The departure of the resultant value of η_0^i from the theoretical prediction is partially caused by the windowing (smoothing) process over the frequency spectra which may cause about 0.3–1.0-MHz broadening in the resultant spectra and has not been taken into account in the fitting process. This can result in at most 10% overes-

TABLE II. The resultant parameters from the least-squares fitting to the Ar plasma. Errors in the last column reflect the uncertainties of the measured values of T_e and N_e.

Parameter	Experiment	Theory ($Z=1$)
κ^i $(\text{sec cm})^{-1}$	$(0.946\pm0.064)\times10^{19}$	$(1.37^{+0.35}_{-0.19})\times10^{19}$
κ^e $(\text{sec cm})^{-1}$	$(3.8\pm2.3)\times10^{21}$	$(2.13^{+0.55}_{-0.30})\times10^{21}$
η_0^i (g/cm sec)	$(3.16\pm0.18)\times10^{-4}$	$(2.26^{+0.58}_{-0.32})\times10^{-4}$
C_{ie} $(\text{sec})^{-1}$	$(2.56\pm0.39)\times10^{7}$	$(2.08^{+0.22}_{-0.39})\times10^{7}$
C_s (cm/sec)	$(2.084\pm0.008)\times10^{5}$	$(2.16^{+0.12}_{-0.07})\times10^{5}$

timation in η_0^i. Besides, the Landau damping, which is not included in the fluid theory, may somewhat broaden the ion-acoustic resonance peak. An estimate based on the result of a computer simulation process gives that η_0^i may be overestimated by at most 5% by not including the effect of Landau damping.

An estimation by Saha's equation shows that about 14% of the particles in the argon plasma are doubly ionized. Because Braginskii theory does not account for more than one ion species, only the first ionization stage is included in the calculations. The ion thermal conductivity estimated by the fitting procedure may be considered as an average value over the first- and second-stage ionized particles. In order to estimate the effects of Ar^{2+} on the average ion thermal conductivity, an effective ion collisional mean free path averaged over all ions is calculated. Considering that the mean path is the weighted average value of the mean paths of all ion species, we have

$$\bar{l}=\frac{\sum_l (N_l / \sum_k N_k Q_{lk})}{\sum_j N_j} ,$$

where N_j is the particle number density of the jth ion species, and Q_{lk} is the collision cross section between particles of species l and k. After simple calculations, we have

$$\bar{l}=l_1 \left[\frac{N_e}{\sum_j N_j} \right] \sum_l \frac{N_l}{\sum_k N_k Z_k^2 Z_l^2 (\ln\Lambda_{kl})/\ln\Lambda_{11})} , \quad (22)$$

where $\ln\Lambda_{kl}$ is the Coulomb logarithm for the Coulomb collisions between ions of species k and l, and l_1 is the mean free path in a pure singly ionized plasma. The effective ion thermal conductivity calculated using the effective mean free path, Eq. (22), given that there are 14% second-stage ionized particles, is 9.5×10^{18} $\sec^{-1}\,\mathrm{cm}^{-1}$, which agrees remarkably well with the result from the fitting process.

The presence of Ar^{2+} species would also affect the values of C_{ie} and η_0^i. The calculated values of C_{ie} and η_0^i using similar approaches are about 16% above and 30% below the predictions for pure singly ionized plasma, respectively. This makes the experimental value of C_{ie} agree with the theoretical prediction better, however, it makes the theoretical value of η_0^i fit the experiment less well.

Because the damping of the ion entropy fluctuations would be dominated by the ion-electron energy-transfer frequency C_{ie} when the wave vector k approaches zero, smaller angle scattering may increase the precision of the resultant value of C_{ie}. Unfortunately, scattering with angles smaller than 2° is difficult in this experiment.

A direct extension of Braginskii's transport equations (two-fluid equations) is made by adding the second-stage ionization species as the third fluid into the theory. Figure 9 presents the predictions of the three-fluid model for the argon plasma, with the third fluid being the 14% second-stage ionization species. In comparison to the predictions by Braginskii two-fluid theory, the three-fluid model predicts narrower entropy-fluctuation peaks, which are closer to the experimental spectra in their shapes, but the ion-acoustic peaks depart even further from the experimental results.

Because of strong interactions between Ar^+ and Ar^{2+} species, the modifications in the spectrum predicted by the two-fluid model in comparison to that predicted by the three-fluid model can be roughly interpreted by a single ion species with some effective (averaged) parameters. A lighter effective mass with respect to unit charge is expected when the Ar^{2+} species is presented, and this results in a larger ion-acoustic velocity. The Ar^{2+} species increases the effective charge number on each ion particle, shortening the ion-ion collision time, and thus resulting in a smaller effective ion thermal conductivity and a larger ion viscosity coefficient.

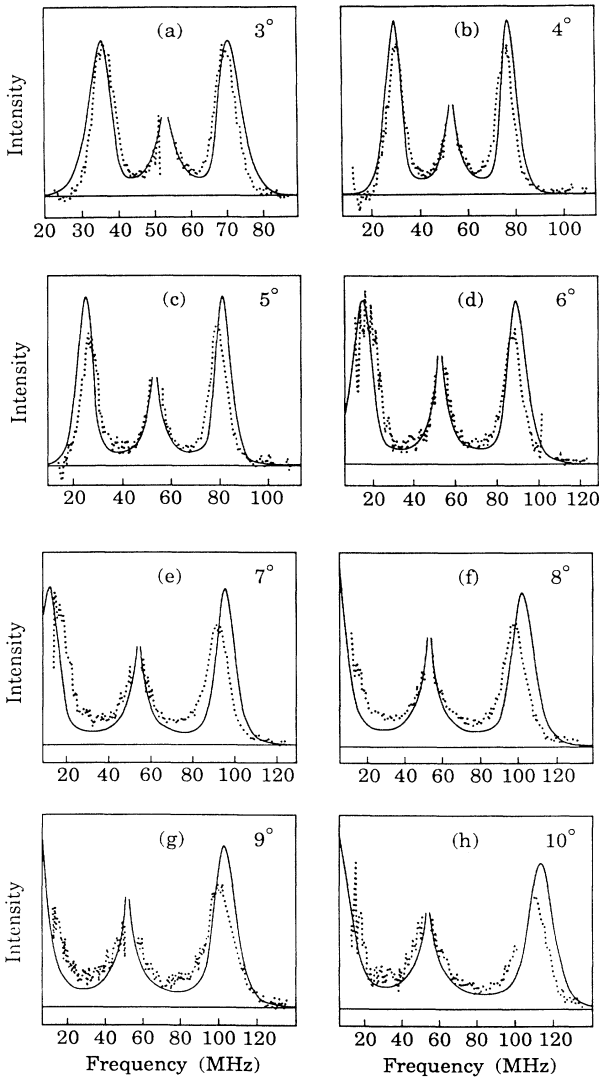

FIG. 9. Data of Fig. 5, with predictions of the three-fluid theory (e^-, A^+, A^{2+}).

C. Conclusions

In summary, we have the following conclusions.

(1) The experimental electron-density fluctuation spectra in both the argon plasma ($N_e=1\times10^{17}$ cm^{-3}, $T_e=2$ eV) and the helium plasma ($N_e=1\times10^{17}$ cm^{-3}, $T_e=2.3$ eV) show the existence of both ion-acoustic resonance peaks and the entropy-fluctuation peak.

(2) The predictions of the Braginskii transport equations, Balescu-Lenard equation, and BGK models agree moderately well with the experimental spectra. The Braginskii theory is valid only when the plasma parameter g is very small, and still fits reasonably to the fluctuation spectrum in the plasmas in this experiment where the plasma parameter $g\simeq0.3$.

(3) The collision processes will reduce the efficiency of Landau damping in the ion-acoustic waves, and the ion-acoustic resonance peak which is heavily Landau damped in a collisionless plasma will be enhanced by the collisions. In a plasma with its ion-ion collision frequency many times greater than the ion-acoustic resonance frequency, the efficiency of the Landau damping will be insignificant in comparison to the other damping mechanisms.

(4) When Landau damping is negligible, the shape of the low-frequency electron-density fluctuation spectrum will be sensitively related to some of the thermal transport coefficients, i.e., ion thermal conductivity, ion viscosity coefficient, collisional ion-electron energy-transfer frequency, and maybe the electron thermal conductivity. The appropriate theory may give the relation of the coefficients to the fluctuation spectrum, and thus may supply a way to estimate the coefficients experimentally through the measurement of the electron-density fluctuation spectrum.

(5) The Braginskii transport equations are adopted as the theory to estimate the transport coefficients experimentally. The least-squares-fitting procedure is used to fit the theoretical spectrum to the experimental data by treating the thermal transport coefficients in the theoretical expression as adjustable, to be determined by the fitting process. This results in the experimental values of the coefficients which are listed in Table II.

(6) Comparison of the experimental values of the coefficients to the predictions of the Braginskii theory is made. Differences are found between the theory and the experiment: ion thermal conductivity κ^i, ion viscosity coefficient η_0^i, and ion-electron energy-transfer frequency C_{ie} resulting from the fitting process are about 30% below, 40% above, and 23% above the theoretical predictions, respectively. The theoretical prediction of ion-acoustic wave phase velocity C_s fits the experiment reasonably.

(7) The Saha equation predicts that the argon plasma in the condition of this experiment contains about 14% doubly ionized particles. An attempt is made to account for the differences between the experiment and the theory, by considering the effect of the second-stage ionization species on the coefficients. The estimate is made by considering an effective ion mean free path and an effective charge number by averaging over first- and second-stage ionization species. The estimate gives -30%, -30%, $+16\%$, and $+6\%$ modifications over the predictions of pure singly ionized plasma for the coefficients κ^i, η_0^i, C_{ie}, and C_s, respectively. This makes the theoretical value of κ^i agree quite well with the experimental value, and of C_{ie} to agree better. However, it causes the theoretical values of η_0^i and C_s to fit the experiment less well.

(8) An attempt is made to add a third fluid into the Braginskii theory in order to include the effect of the 14% second-stage ionization species. This results in an electron-density fluctuation spectrum with its entropy peak fitting the experimental data better, but its ion-acoustic peak departing further from the experimental data. This is equivalent to the results obtained by averaging the thermal transport coefficients over singly and second-stage ionized particles as mentioned above.

(9) The two-species BGK model introduced previously, which includes the collisional interactions between the ions and electrons, has a better fit to the experimental spectrum in comparison to the ordinary BGK model. Broader ion-acoustic and entropy peaks predicted by the two-species BGK model than that by the ordinary BGK model show that the collisional interactions will increase the damping in both the ion-acoustic waves and the entropy fluctuations. This is consistent with the results of the Braginskii theory. In addition, the entropy-fluctuation peak predicted by the two-species BGK agrees with the experimental results better than that predicted by Braginskii's equations. However, the two-species BGK model still gives narrower ion-acoustic resonance peaks in comparison to the experimental results. This departure of the theory from the experiment may be related to the simplifications of the Coulomb collisions in the BGK collision terms.

ACKNOWLEDGMENTS

The authors gratefully acknowledge the many contributions of Dr. A. N. Mostovych to this work. This work was supported by NSF.

[1] A. N. Mostovych, Ph.D. thesis, University of Maryland at College Park, 1984.

[2] A. N. Mostovych and A. W. DeSilva, Phys. Rev. Lett. **53**, 1563 (1984); Phys. Rev. A **34**, 3238 (1986).

[3] Y. Q. Zhang, A. W. DeSilva, and A. N. Mostovych, Phys. Rev. Lett. **62**, 1848 (1989).

[4] S. I. Braginskii, in *Reviews of Plasma Physics,* edited by M. A. Leontovich (Consultants Bureau, New York, 1964).

[5] R. Kubo, in *Lectures on Theoretical Physics,* edited by W. E. Brittin and L. G. Dumham (Interscience, New York, 1959), Vol. I.
[6] H. B. Callen and T. A. Welton, Phys. Rev. **83**, 34 (1951).
[7] S. Ichimaru, *Basic Principles of Plasma Physics, A Statistical Approach* (Benjamin/Cummings, New York, 1973).
[8] P. L. Bhatngar, E. P. Gross, and M. Krook, Phys. Rev. **94**, 511 (1954).
[9] A. A. Galeev and R. N. Sudan, *Basic Plasma Physics* (North-Holland, New York, 1983).
[10] Y. Q. Zhang, Ph.D. thesis, University of Maryland at College Park, 1989.
[11] A. W. DeSilva and G. C. Goldenbaum, *Methods of Experimental Physics* (Academic, New York, 1970), Vol. 9, Part A.
[12] H. Z. Cummins and H. L. Swinney, in *Progress in Optics,* edited by E. Wolf (North-Holland, New York, 1970), Vol. 8.